^{14}CO was not injected into the reactor. Correction for this relatively small effect can be made by subtracting the lowest OH concentrations measured that day from all the higher concentrations, because models consistently predict night-time OH concentrations less than 10^5 radicals cm^{-3}. These corrections, usually equivalent to less than 2.5×10^5 radicals cm^{-3}, have not been made in the present data. The precision of the results can also be estimated by comparing the data for 1, 2 and 7 October with those for 14 and 15 October; very similar results were obtained on days with comparable meteorological and chemical conditions.

These results are significant because the low $^{14}CO_2$ levels in the early morning and evening suggests that the elevated midday $^{14}CO_2$ levels are caused by the photochemical reaction between CO and OH. Experiments in which the reactor was shielded from ultraviolet radiation (Fig. 1) yielded OH concentrations which were slightly smaller than adjacent unshielded values, suggesting that the primary OH source is the HO_2–NO reaction. Weinstock *et al.*[32] show that the OH concentrations do not decay completely within the reaction time upon ultraviolet flux interruption.

A more detailed presentation of the method, results and model comparisons will be made elsewhere. Future improvements for this method include increased separation of ^{222}Rn from the $^{14}CO_2$ and reduction of the sample integration time to 25 s. With complete radon removal, a detection limit of 10^4 radicals cm^{-3} is feasible, enabling night-time detection of OH. In contrast to laser techniques, limitations of the radiochemical technique are determined by operations performed in the laboratory. Improvements in separation efficiency can be made at low cost and will result in a proportionately lower detection limit until counting becomes limiting at about 10^4 radicals cm^{-3}. Laser methods, however, are limited primarily by uncontrollable atmospheric fluctuations. Also, the integration time of 100 s is much less than that required for laser methods[14,15,17,18], which average signals for several hours in the course of a single OH measurement. Just as local measurements are preferable to global measurements in elucidating basic atmospheric chemistry, there is great value in a measurement time approaching the lifetime of the species of interest.

This work was partially supported by the Washington State University College of Engineering, the NSF and NASA grants. We also acknowledge the help of Harbi Elshafei, J. Carl Farmer and Yvonne Welter.

Received 18 April; accepted 18 July 1988.

1. Levy, H. *Science* **173**, 141-143 (1971).
2. Perner, D. *et al. J. atmos. Chem.* **5**, 185-216 (1987).
3. Logan, J. A., Prather, M. J., Wofsy, S. C. & McElroy, M. B. *J. geophys. Res.* **86**, 7210-7254 (1981).
4. Singh, H. B. *Geophys. Res. Lett.* **4**, 453-456 (1977).
5. Neely, W. B. & Plonka, J. H. *Envir. Sci. Technol.* **12**, 317-321 (1978).
6. Fraser, P. J., Hyson, P., Rasmussen, R. A., Crawford, A. J. & Khalil, M. A. K. *J. atmos. Chem.* **4**, 3-42 (1986).
7. Baardson, E. L. & Terhune, R. W. *Appl. Phys. Lett.* **21**, 209-211 (1972).
8. Wang, C. C. & Davis, L. I. *Phys. Rev. Lett.* **32**, 349-352 (1974).
9. Davis, L. I. *et al. J. geophys. Res.* **92**, 2020-2024 (1987).
10. Davis, D. D., Heaps, W. & McGee, T. *Geophys. Res. Lett.* **3**, 331-333 (1976).
11. Davis, D. D., Heaps, W., Philen, D. & McGee, T. *Atmos. Envir.* **13**, 1197-1203 (1979).
12. Hard, T. M., O'Brien, R. J., Cornelius, Y C. & Mehrabzadeh, A. A. *Envir. Sci. Technol.* **18**, 768-777 (1984).
13. Hard, T. M., Chan, C. Y., Mehrabzadeh, A. A., Pan, W. H. & Obrien, R. J. *Nature* **322**, 617-620 (1986).
14. Shirinzadeh, B., Wang, C. C. & Deng, D. Q. *Geophys. Res. Lett.* **14**, 123-126 (1987).
15. Ortigies, G., Gericke, K.-H. & Comes, F. J. *Z. Naturf.* **86a**, 177-183 (1981).
16. Wang, C. C., Davis, L. I., Selzer, P. M. & Munoz, R. *J. geophy. Res.* **86**, 1181-1186 (1981).
17. Davis, D. D., Rodgers, M. O., Fischer, S. D. & Heaps, W. S. *Geophys. Res. Lett.* **8**, 73-76 (1981).
18. Perner, D. *et al. Geophys. Res. Lett.* **8**, 466-468 (1976).
19. Platt, U., Rateike, M., Junkermann, W., Hofzumahaus, A. & Ehhalt, D. H. *Free Radical Res. Commun.* **3**, 165-172 (1987).
20. Campbell, M. J., Sheppard, J. C. & Au, B. F. *Geophys. Res. Lett.* **6**, 175-178 (1979).
21. Sheppard, J. C., Hardy, E. J. & Hopper, F. *Antarct. J. U.S.* **17**, 206-207 (1982).
22. Campbell, M. J. *et al. J. atmos. Chem.* **4**, 413-427 (1987).
23. Hynes, A. J., Wine, P. H. & Ravishankara, A. R. *J. geophys. Res.* **91**, 11815-11820 (1986).
24. Hardy, R. J., Sheppard, J. C. & Campbell, M. J. *Int. J. appl. Radiat. Isotopes* **35**, 1071-1072 (1984).
25. Farmer, J. C., Fitzner, C. A., Campbell, M. J., Henry, M. N. & Sheppard, J. C. *Int. J. appl. Radiat. Isotopes* **36**, 915-918 (1985).
26. Felton, C. C. thesis, Washington State Univ. (1988).
27. Zafonte, L., Rieger, P. L. & Holmes, J. R. *Envir. Sci. Technol.* **11**, 483-487 (1977).
28. Meyn, L. A. thesis, Washington State Univ. (1982).
29. Hoell, J. M. *et al. J. geophys. Res.* **89**, 11819-11825 (1984).
30. Sheppard, J. C. College of Engineering Bulletin 338, Washington State Univ. (1975).
31. Demerjian, K. L., Schere, K. L. & Peterson, J. T. *Adv. Envir. Sci. Technol.* **10**, 369-459 (1980).
32. Weinstock, B., Niki, H. & Chang,. T. Y. *Adv. Envir. Sci. Technol.* **10**, 221-258 (1980).

Surface electronic properties probed with tunnelling microscopy and chemical doping

Xian-Liang Wu, Peng Zhou & Charles M. Lieber*

Department of Chemistry, Columbia University, New York 10027, USA

Scanning tunnelling microscopy[1–3] (STM) can provide atomic-resolution images of surfaces in vacuum[4,5], air[6] and liquids[7,8]. One of the most appealing aspects of such images is that they appear to reflect surface structure directly; these tunnelling images, however, contain contributions from both the structural and the electronic properties of a surface[1–5]. Although an understanding of these properties is essential to an understanding of the fundamental nature and reactivity of surfaces, few methods[5] are available to separate them, especially in air and in liquids. Here we report a new approach to this problem that combines chemical modifications with tunnelling microscopy. Samples of the layered material tantalum disulphide (TaS_2) have been substitutionally doped with titanium to prepare materials of the general form $Ti_xTa_{1-x}S_2$. STM images of native TaS_2 are dominated by a charge density wave state[9–11]. Using titanium doping, we have been able to perturb this unusual electronic feature systematically so that the surface structure can be imaged clearly. Such studies of chemically modified materials (prepared, for example by doping or intercalation) should lead to a better understanding of the features contained in STM images.

Tantalum disulphide is a member of the transition metal dichalcogenides, a group of layered materials that exhibit interesting electrical, magnetic and catalytic properties[12,13]. The highly anisotropic structure of TaS_2 consists of covalent S–Ta–S layers that are bonded together weakly, predominantly by van der Waals interactions (Fig. 1*a*). The sulphur and tantalum centres are arranged in hexagonal close-packed (h.c.p.) planes with $a_0 = 3.35$ Å. Our studies concentrate on crystals in which the tantalum centres are coordinated in octahedral holes, although octahedral or trigonal prismatic coordination is possible. A unique feature of octahedrally coordinated TaS_2 is its charge density wave (CDW) state, a temperature-dependent periodic distortion of the lattice and the electron density within the S–Ta–S layers. The lattice distortions are small (<0.2 Å) but the periodic variation of the electron density is quite large (11.7 Å) (ref. 13).

Single crystals of TaS_2, grown by chemical vapour transport using I_2, can be cleaved along the *a*-axis to expose large atomically flat regions of h.c.p. sulphur atoms[9]. A typical tunnelling image of such a surface, recorded in the constant current mode using our STM, is shown in Fig. 2. A hexagonal lattice is prominent in this surface image, but the peak spacing and corrugation are 11.8 ± 0.2 and 5.7 ± 0.5 Å respectively, much larger than the values expected for the h.c.p. sulphur plane (3.35 and <1 Å respectively)[14]. The features observed in this STM image are due to the periodic variation in charge associated with the CDW state in TaS_2[9–11]. Although there is no atomic structure visible in this image, we and others have observed such structure occasionally in other experiments (Lieber *et al.*,

* To whom correspondence should be addressed.

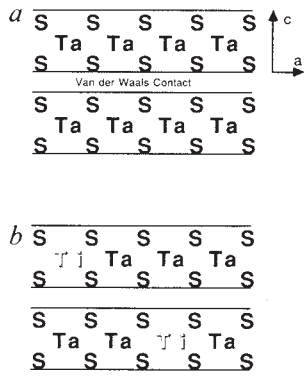

Fig. 1 Cross-sectional veiw of the structure of tantalum disulphide which displays two S-Ta-S layers in van der Waals contact. *b*, Tantalum disulphide substitutionally doped with titanium. The titanium-doped material is prepared by reaction of the appropriate ratio of metals and sulphur $(x\mathrm{Ti}+(1-x)\mathrm{Ta}+2\mathrm{S})$ at 950 °C.

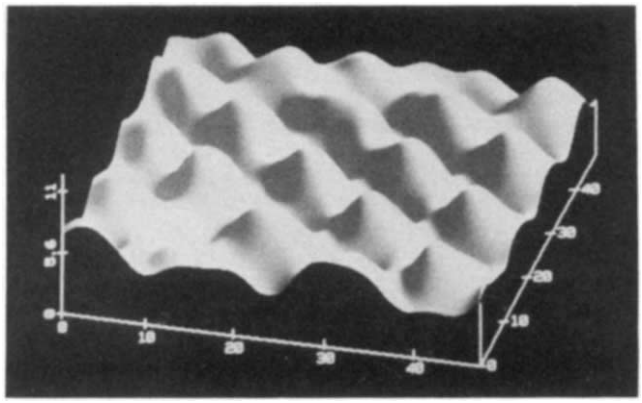

Fig. 2 STM image of TaS_2 recorded at room temperature using a modified commercial instrument (Digital). The image was recorded in the constant current mode (tunnelling current 2.1 nA) with a platinum-iridium alloy (90%-10%) tip biased at +26 mV relative to the sample. The sample surface was covered with oil (Fluorolube, Fisher Scientific), although similar images were also obtained in air. The raw digital data was low-pass-filtered before display. The axes markings are in Å.

Clarke *et al.* and Coleman *et al.*, unpublished results); nevertheless, it is difficult to observe the atomic lattice directly because of the strong CDW signal.

Knowledge of both the electronic and structural properties of a surface are necessary to understand certain characteristics, such as its reactivity. Spectroscopic tunnelling measurements have been used successfully to delineate these properties in ultrahigh vacuum[5], but such measurements are difficult to carry out in air and liquid environments. To obtain this crucial infor mation we have been developing methods based on well-define chemical modifications that perturb the electronic properties of the surface without changing its structure[11]. By imaging a series of chemically modified materials one can obtain a more complete understanding of the electronic and structural nature of a surface.

Randomly doped samples of $Ti_xTa_{1-x}S_2$, where $x = 0.06$ and 0.1 (ref. 15), are used here (Fig. 1*b*). Although titanium doping decreases the average electron density by one electron per Ti atom, the structure of the modified material is virtually the same as the parent TaS_2. STM images of these two samples are shown in Fig. 3. These images are typical of the many (>40) we have obtained at different locations on several different samples using different tips. It is readily apparent from Fig. 3 that even low levels of Ti-doping perturb the CDW state sufficiently that the atomic lattice can be 'seen' clearly. For the $x = 0.06$ sample, the

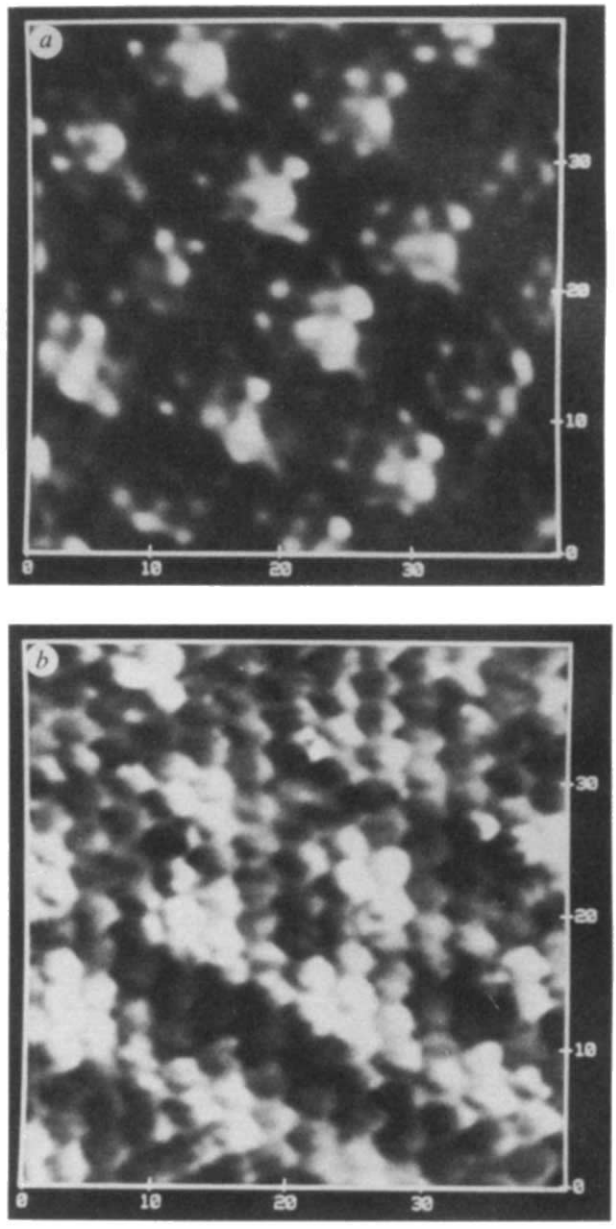

Fig. 3 Grey-scale images of $Ti_xTa_{1-x}S_2$ recorded in the constant current mode. The sample surfaces were covered with oil to improve the imaging stability[17]. *a*, $x = 0.06$; tip bias = +8 mV, tunnelling current = 2.1 nA. The grey-scale in this image (black minimum to white maximum) is 4.3 Å. *b*, $x = 0.1$; tip bias voltage +9 mV, tunnelling current = 2.1 nA. The grey-scale in this image, 2.9 Å, is significantly smaller than in *a*. The *x*, *y*-axes markings are in Å.

CDW is still prominent as large peaks (11.6 ± 0.2 Å peak-to-peak separation and 3.6 ± 0.5 Å corrugation), but examination also reveals smaller satellite peaks with separation 3.3 ± 0.1 Å, which we assign to the h.c.p. sulphur atoms. For $x = 0.1$ samples (Fig. 3*b*) the atomic lattice, with peak-to-peak separation 3.4 ± 0.1 Å, dominates the tunnelling images; the CDW is visible only as a weak periodic ~11.6 Å modulation of the sulphur atoms (1.4 ± 0.4 Å corrugation). The corrugations measured indicate that the CDW amplitude decreases substantially with increasing dopant concentration. Because some variation in corrugation is found for a given titanium concentration, we have analysed the corrugations from at least 15 images for each dopant concentration to determine whether this trend is significant. The images were recorded with similar instrumental parameters (bias voltage and tunnelling current). We find that the corrugations ($\pm 1\sigma$) for

$x = 0$, 0.06 and 0.10 are 5.2 ± 0.9, 3.5 ± 0.6 and 1.2 ± 0.3 Å respectively, which demonstrates that the observed effect of Ti-doping is greater than the sample-to-sample variation for a given titanium concentration. In related work Coleman *et al.* have shown[16] that the CDW amplitude decreases with increasing tunnelling current, but even at high currents no atomic structure was reported.

Although Ti-doping clearly modifies the electronic properties of TaS_2 sufficiently to enable STM to probe the surface structure, the origin of these effects is not certain. Doping with titanium causes randomness in the lattice potential and decreases the conduction-electron density by one electron per Ti atom (substituting $d^0 - Ti$ for $d^1 - Ta$)[12,13]. These two effects will perturb the CDW in different ways. Disorder in the potential suppresses the temperatures at which the CDW, which is incommensurate with the lattice at high temperatures, undergoes transitions first to a quasicommensurate and then to a commensurate state. For $x = 0$, 0.06 and 0.1 the incommensurate to quasicommensurate transition temperatures are ~350, 305 and 250 K, respectively[15]. Hence, at our experimental temperature (295 K) the CDW is quasicommensurate with the lattice of TaS_2, close to a transition for $Ti_{0.06}Ta_{0.94}S_2$, and incommensurate with the lattice of $Ti_{0.1}Ta_{0.9}S_2$. Because the CDW amplitude increases in the quasicommensurate state[13], we believe that the increase in observed atomic structure with increasing Ti is probably due to a decrease in the CDW amplitude associated with the incommensurate state. We are engaged in experiments designed to probe this point further.

On the other hand, a decrease in the conduction electron density will cause the Fermi surface to shrink (in the rigid-band approximation) and hence the CDW wavelength should increase[12,13]. Diffraction studies[15] suggest that for the $x = 0.1$ sample the CDW modulation should be 12.5 Å (as opposed to 11.7 Å for $x = 0$), but we observe no such change. It is not clear why the change in conduction electron density does not appear to affect the wavelength of the CDW determined from the STM images. But we note that our STM results probe the local charge modulation directly whereas diffraction studies measure the lattice distortions that are coupled to the CDW. Clearly more work is needed to understand these effects.

In conclusion, our results demonstrate how chemical modifications can be combined with tunnelling microscopy to separate the electronic and structural components of STM surface images. Such well defined chemical methods should be useful for studies of other low-dimensional materials (such as graphite and M_xWO_3) that can be modified by intercalation, doping and other methods. Such studies are currently in progress in our laboratory.

We thank F. J. DiSalvo and C. J. Chen for discussion, the referees for bringing to our attention unpublished work, and J. V. Waszczak for supplying titanium-doped samples. This work was partially supported by Presidential Young Investigator and Dreyfus New Faculty Awards (C.M.L.).

Received 30 May; accepted 20 July 1988.

1. Binnig, G. & Rohrer, H. *Angew. Chem., int. Ed. Engl.* **26,** 606–614 (1987).
2. Hansma, P. K. & Tersoff, J. *J. appl. Phys.* **61,** R1–R23 (1987).
3. Quate, C. F. *Physics Today* **39,** 26–33 (1986).
4. Becker, R. S. *Proc. natn. Acad. Sci. U.S.A.* **84,** 4667–4670 (1987).
5. Tromp, R. M., Hamers, R. J. & Demuth, J. E. *Science* **234,** 304–309 (1986).
6. Park, S.-I. & Quate, C. F. *Appl. Phys. Lett.* **48,** 112–114 (1986).
7. Sonnenfeld, R. & Hansma, P. K. *Science* **232,** 211–213 (1986).
8. Giambattista, B. *et al. Proc. natn. Acad. Sci. U.S.A.* **84,** 4671–4674 (1987).
9. Coleman, R. V., Drake, B., Hansma, P. K. & Slough, G. *Phys. Rev. Lett.* **55,** 394–397 (1985).
10. Slough, C. G., McNairy, W. W., Coleman, R. V., Drake, B. & Hansma, P. K. *Phys. Rev. B* **34,** 994–1005 (1986).
11. Wu, X.-L. & Lieber, C. M. *J. Am. chem. Soc.* **110,** 5200 (1988).
12. Wilson, J. A., DiSalvo, F. J. & Mahajan, S. *Adv. Phys.* **24,** 117–201 (1975).
13. DiSalvo, F. J. in *Electron-Phonon Interactions and Phase Transitions*, (ed. Riste, T.) 107–136 (Plenum, New York, 1977).
14. Slough, C. G. *et al. Phys. Rev.* B **37,** 6571–6574 (1988).
15. DiSalvo, F. J., Wilson, J. A., Bagley, B. G. & Waszczak, J. V. *Phys. Rev. B* **12,** 2220–2235 (1975).
16. Coleman, R. V. *et al. J. Vac. Sci. Technol.* A **6,** 338–343 (1988).
17. Schneir, J. & Hansma, P. K. *Langmuir* **3,** 1025–1027 (1987).

Contaminated aquifers are a forgotten component of the global N_2O budget

Daniel Ronen*†, Mordeckai Magaritz* & Ehud Almon*

* Isotope Department, The Weizmann Institute of Science, 76100 Rehovot, Israel
† Research Department, Hydrological Service, PO Box 6381, Jerusalem 91063, Israel

One of the chemical components contributing to the destruction of the ozone layer in the upper atmosphere consists of the nitrogen oxides formed from N_2O (ref. 1). Prompted by the prevailing idea that the ocean is not a major source of N_2O or a sink for N_2O, estimates have been made of global fluxes from continental ecosystems[2]. Although most land areas are underlain by groundwater[3], this medium has never been considered in global budgeting of N_2O. A large number of aquifers around the world are contaminated by nitrogen compounds, and processes of nitrification and denitrification are reported to be operative in this environment[3]. These processes lead to the production of N_2O (refs 4 and 5). Here we report that the concentration of N_2O in phreatic aerobic aquifers contaminated by anthropogenic activities (disposal of human or animal waste, cultivation and fertilization) are up to three orders of magnitude higher than the concentration expected as a result of equilibrium with the atmosphere.

Water samples were collected in the Netherlands and Israel (1) at the Veluwe region (52°15′ N, 5°40′ W), where a shallow 9 m-deep sandy aquifer under woodland is contaminated by

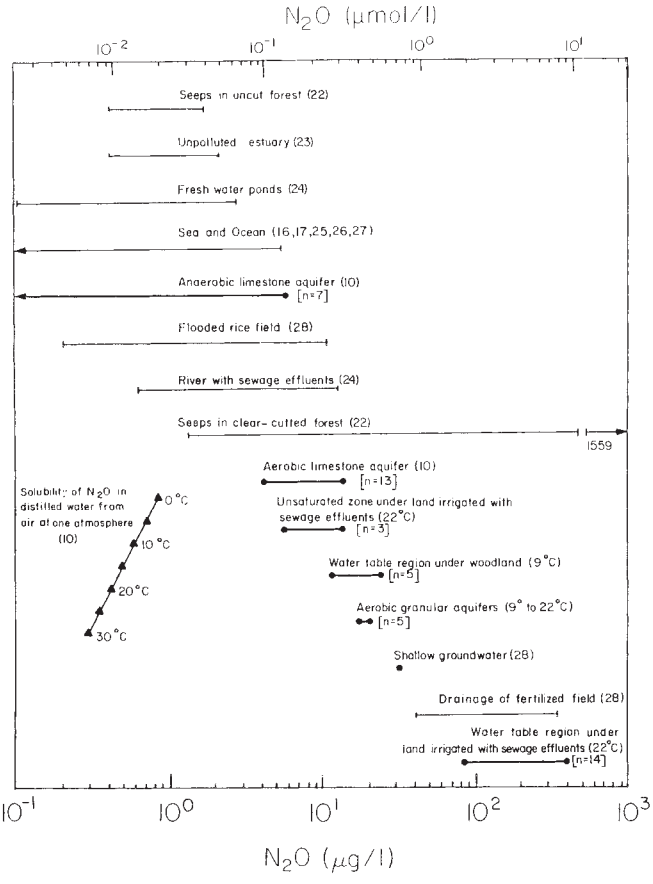

Fig. 1 Concentration range of N_2O in different aquatic systems. The theoretical solubility of N_2O at different temperatures is also given. The concentration ranges of N_2O in aquifer systems obtained during this study are denoted by filled circles. The number of samples is given by *n*. Numbers in parentheses are references.